Progress In Electromagnetics Research M, Vol. 87, 127–136, 2019

Gain Enhancement in MIMO Antennas Using Defected Ground Structure

Nguyen N. Lan[1, 2, *]

Abstract—This paper investigates a low-profile Multiple Input Multiple Output (MIMO) antenna with enhanced gain based on Defected Ground Structure (DGS). The proposed antenna consists of two sets of four elements (2×2), and it is yielded at the central frequency of 5.5 GHz for Wireless Local Area Network (WLAN) applications. Being on RT5880 with height of 1.575 mm, the overall dimensions of MIMO antenna and single array are $145 \times 88 \times 1.575\,\text{mm}^3$ and $75 \times 82 \times 1.575\,\text{mm}^3$, respectively. To get high gain and low mutual coupling for antenna, a Defected Ground Structure (DGS) is proposed and integrated on ground plane. At 5.3 GHz, the gain of antenna achieves approximately 9.5 dBi while mutual coupling level is under -20 dB. Besides, the MIMO antenna witnesses a radiation efficiency of 93%. The measurement results are compared to simulation ones to verify the performance of the proposed antenna.

1. INTRODUCTION

Nowadays, microstrip antennas have attracted interest from researchers because of their characteristics of low cost, compact size, easy fabrication, and integration. However, to meet practical applications, microstrip antennas are expected to achieve higher gain and radiation efficiency. To enhance the gain for antenna, different approaches have been reported, for example: DGS [1, 2], loading method [3], superstrate [4, 5], reflective surface [6], and metamaterial [7, 8]. Although superstrate and some other methods considerably improve gain for antenna, they increase the complexity and occupied space. In addition, they also raise the cost of antenna. Meanwhile, method of reflective surface enhances gain for antenna based on reflection principle to reduce side lobe and back lobe. However, it leads to increasing occupied space. Therefore, one of the easiest methods to improve gain for antenna is using DGS [9]. DGS is realized by connecting the regular Photonic-Bandgap Structures (PBG) with narrower slots in the ground plane [10]. By adjusting DGS dimensions, the resonant frequency can be changed.

Besides, the demand on high data rates and high reliability is extremely exigent. With benefits such as high data rate, high reliability and spectral efficiency with the same bandwidth and power level, Multiple Input Multiple Output (MIMO) technology is the best solution to meet the aforementioned requirements [11]. However, when antennas in a MIMO system are placed closer, the phenomenon of mutual coupling appears.

Mutual coupling is the electromagnetic interaction between antennas in an array. Mutual coupling is an undesired phenomenon because energy is transmitted by an antenna and absorbed by other antennas. This leads to waste in energy. Moreover, mutual coupling not only causes reducing radiation efficiency of antenna, but also affects correlation as well.

Recently, there are a lot of published papers to improve parameters for MIMO antennas, and they have been proposed in [12–15]. However, gain values of these antenna are quite low while the isolation

Received 11 September 2019, Accepted 25 November 2019, Scheduled 16 December 2019

* Corresponding author: Nguyen N. Lan (nnlan@moet.edu.vn).

[1] Institute of Research and Development, Duy Tan University, Danang 550000, Vietnam. [2] Faculty of Electronics and Telecommunications, Saigon University, Vietnam.

ones are under −16 dB. In detail, the gain values in [12] and [13] are very low (under 2 dBi). In addition, the bandwidth percentage of antenna in [13] is only 2%. Similarly, although there is a large bandwidth percentage in [15], the gain and isolation of antenna are not good (4 dBi and 14 dB).

In this paper, a MIMO antenna including two sets of four elements (2 × 2), having a good isolation with the distance from edge to edge of 1.65 mm, is presented. Moreover, to achieve high gain and radiation efficiency, a new DGS is proposed and integrated on ground plane. The antenna is yielded at the central frequency of 5.3 GHz for WLAN applications based on RT5880 with dielectric constant of 2.2. The antenna is designed, simulated, and optimized by using Computer Simulation Technology Microwave Studio (CST MS). The performance of the proposed antenna is investigated through simulation and measurement, and the measured results are compared with the simulated ones.

2. PRINCIPLE OF THE GAIN ENHANCEMENT BY USING DEFECTED GROUND STRUCTURE

We know that for a microstrip antenna, there is a current redistribution when DGS is used on ground plane, and this causes an interference between waves. This current redistribution opens an opportunity in gain enhancement for the antenna. Now, we consider two Gaussian waves, then the expressions for the electric field of two waves are given by [16]:

$$E_1 = E_0\hat{x}\frac{W_0}{W(z)}e^{-\frac{r^2}{W(z)^2}}e^{-i\left(kz+k\frac{r^2}{2R(z)}-\psi(z)+\varphi_1\right)} \tag{1}$$

$$E_2 = E_0\hat{x}\frac{W_0}{W(z)}e^{-\frac{r^2}{W(z)^2}}e^{-i\left(kz+k\frac{r^2}{2R(z)}-\psi(z)+\varphi_2\right)} \tag{2}$$

$$w(z) = \omega_0\sqrt{1+\left(\frac{z}{z_R}\right)^2} \tag{3}$$

$$z_R = \frac{\pi\omega_0^2}{\lambda} \tag{4}$$

$$R(z) = z\left[1+\left(\frac{z_R}{z}\right)^2\right] \tag{5}$$

$$\psi(z) = arctan\left(\frac{z}{z_R}\right) \tag{6}$$

Then, the total electric field can express as following:

$$\begin{aligned} E_t &= E_1+E_2 = 2E_0\hat{x}\frac{W_0}{W(z)}2e^{\left(-\frac{r^2}{W(z)^2}\right)}\left[\cos\left(kz+k\frac{r^2}{2R(z)}-\psi(z)+\left(\frac{\varphi_1+\varphi_2}{2}\right)\right)\cos\left(\frac{\varphi_1-\varphi_2}{2}\right)\right. \\ &\quad \left.+isin\left(kz+k\frac{r^2}{2R(z)}-\psi(z)+\left(\frac{\varphi_1+\varphi_2}{2}\right)\right)\cos\left(\frac{\varphi_1-\varphi_2}{2}\right)\right] \\ &= 4E_0\hat{x}\frac{W_0}{W(z)}e^{\left(-\frac{r^2}{W(z)^2}\right)}\cos\left(\frac{\varphi_1-\varphi_2}{2}\right)e^{-i\left(kz+k\frac{r^2}{2R(z)}-\psi(z)+\left(\frac{\varphi_1+\varphi_2}{2}\right)\right)} \end{aligned} \tag{7}$$

And the magnetic field can be written:

$$H_t = \frac{1}{\mu}4E_0\hat{y}\frac{W_0}{W(z)}e^{\left(-\frac{r^2}{W(z)^2}\right)}\cos\left(\frac{\varphi_1-\varphi_2}{2}\right)e^{-i\left(kz+k\frac{r^2}{2R(z)}-\psi(z)+\left(\frac{\varphi_1+\varphi_2}{2}\right)\right)} \tag{8}$$

Finally, Poynting vector is defined by:

$$S_t = \vec{E}\times\vec{H} = \frac{1}{\mu}\vec{E}\times\vec{H} = \frac{16}{\mu}E_0^2\hat{z}\left(\frac{W_0}{W(z)}\right)^2 e^{\left(-\frac{r^2}{W(z)^2}\right)^2}\cos^2\left(\frac{\varphi_1-\varphi_2}{2}\right)e^{-2i\left(kz+k\frac{r^2}{2R(z)}-\psi(z)+\frac{\varphi_1+\varphi_2}{2}\right)} \tag{9}$$

with μ being the permeability of medium.

From Equation (9), we can see that the Poynting vector depends on the phase difference between two Gaussian waves ($\cos^2\left(\frac{\varphi_1-\varphi_2}{2}\right)$). Here, Poynting vector reaches maximum value when there is no phase difference between waves ($\varphi_1 - \varphi_2 = 0$). In contrast, if the phase shift between waves is odd multiple of π, then the value of Poynting vector is 0. Therefore, the gain of antenna is only enhanced when we redistribute current in order that more and more currents at the place of the phase shift are 0 whereas there is a limitation in other places.

3. THE PROPOSED ANTENNA ARRAY

3.1. Design of Array Antenna

There are a lot of different shapes of geometries embedded on the ground plane under the microstrip line. The shape of the proposed DGS is started from rectangular dumbbell in [17]. By replacing and modifying in the structure shape, the paper gets a new structure as shown Fig. 1. The proposed structure consists of two hexagon shapes, and they are connected with each other by a microstrip line. Meanwhile, the square (inside the hexagon shape) is truncated at four corners, and they are linked to hexagon shapes by microstrip lines. By using DGS integrated on ground plane, parasitic capacitors are made, and then, the equivalent circuit of the structure is displayed in Fig. 1(b). This structure is applied to an antenna array (2 × 2), and its model is shown in Fig. 2. The antenna is designed for WLAN applications at central frequency of 5.3 GHz. It includes four microstrip patches on the

(a) (b)

Figure 1. (a) The proposed model of DGS; (b) equivalent circuit (dark colour for metal and light colour for substrate).

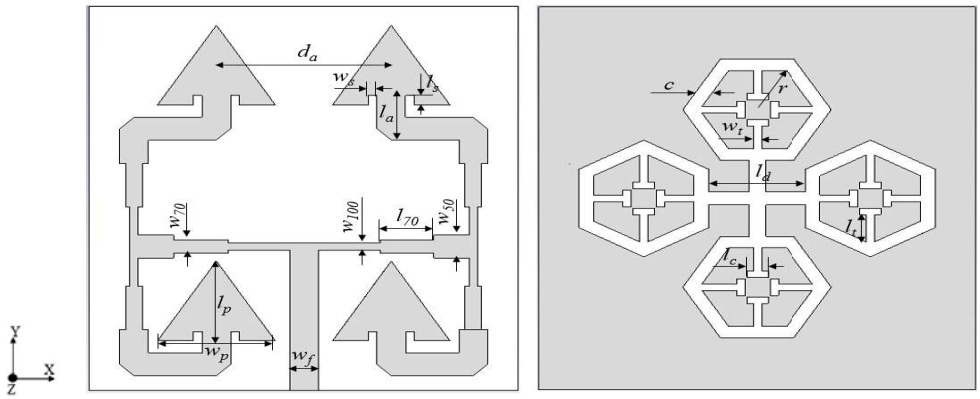

(a) (b)

Figure 2. Geometry of the microstrip antenna: (a) front; (b) rear.

substrate, which are connected through three power dividers. Based on a Roger RT/Duroid^{TM} 5880 substrate with $h = 1.575\,\text{mm}$, $\varepsilon_r = 2.2$, and $\tan\delta = 0.0009$, the total size of antenna array is $75 \times 82 \times 1.575\,\text{mm}^3$ while the distance from patch center to patch center is approximately $\lambda/2$ (λ is the wavelength in free space). Meanwhile, based on formulas in [18] the proposed antenna gets a patch size of $20 \times 17\,\text{mm}^2$. The other part of antenna on the backside of the substrate is ground plane integrated DGS. Table 1 shows the design parameters of antenna.

Table 1. The design parameters of the proposed antenna (mm).

l_p	w_p	w_f	w_{100}	w_{70}	l_{70}	w_s	l_s
18.025	20.6	4.9	1.45	2.85	9	1.2	1.8
l_a	d_a	c	r	w_t	l_d	l_t	l_c
9.3	28	3.2	12.5	1.6	20	6.5	3.8

3.2. Design of MIMO antenna

The model of MIMO antenna is illustrated in Fig. 3. The MIMO antenna consists of two arrays placed side by side on top in the substrate, in which each array includes four elements (2×2). The overall dimension of antenna is $145 \times 88 \times 1.575\,\text{mm}^3$, whereas the distance from edge to edge of the two arrays is 1.65 mm. Currently, there are many different configurations that can be used to feed microstrip antennas, for example: microstrip line, coaxial probe, aperture coupling, and proximity coupling. The method of microstrip feed line is the most popular methods thanks to its ease in design, fabrication, and impedance matching. Therefore, it is chosen to feed antenna elements in this paper.

Besides, to enhance antenna gain, a new DGS is proposed, and it is etched on ground plane. By etching DGS on ground, the characteristics of a transmission line are changed such as resistance, capacitance, and inductance. Then, the resonant frequency of the DGS depends on some factors: shape,

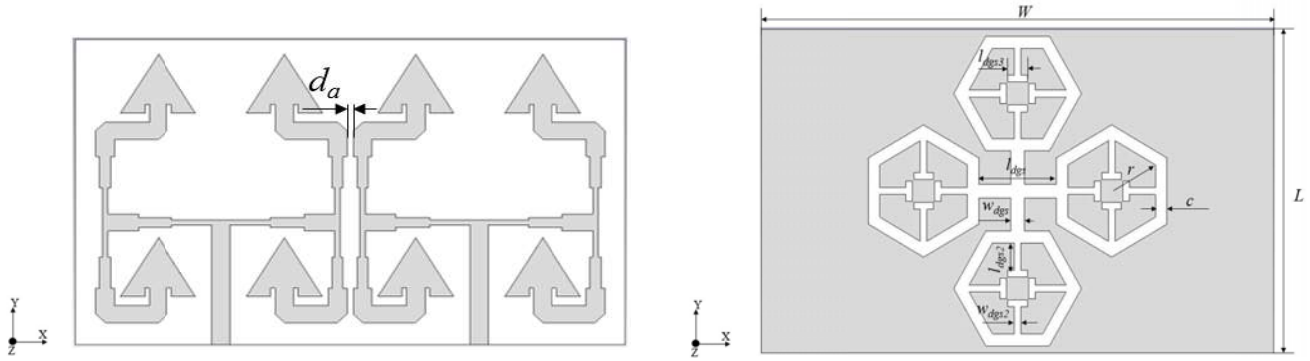

(a) (b)

Figure 3. The model of the proposed MIMO antenna: (a) front and (b) rear.

Table 2. Some parameters of the proposed MIMO antenna (mm).

W	L	d_a	r	c
145	88	1.65	18	3.8
w_{dgs}	l_{dgs}	w_{dgs2}	l_{dgs2}	l_{dgs3}
3.8	24	1.9	10	2.25

etching place, and size of DGS, and these factors can be satisfied by adjusting some parameters of DGS: c, r, l_d, l_t, w_t, l_c. For this reason, two DGSs (as shown in Fig. 1) which are placed orthogonal to each other are selected in this paper. Moreover, for an easy fabrication and design, the proposed DGS is located at the center of the ground. Table 2 exhibits some parameters of the proposed MIMO antenna.

4. RESULTS AND DISCUSSION

4.1. Simulated Results

4.1.1. Single Array Antenna

Firstly, Fig. 4 illustrates the reflection coefficient of the proposed single antenna. It is obvious that the percentage of bandwidth is 11.8% corresponding to 624 MHz. We know that the bandwidth percentage of a regular microstrip antenna is only 5–6%. This shows that the bandwidth percentage of antenna is significantly improved. Currently, there are many methods to expand bandwidth for antenna, and one of ways is the creation of multiple consecutive resonant modes. In Fig. 4, there are two created resonant modes for bandwidth of antenna. As a result, the bandwidth of antenna is extended. Making consecutive resonant modes not only enhances bandwidth for antenna, but also makes radiation efficiency remain at high level. This is shown while the gain and radiation efficiency of the single array antenna achieve 8.5 dBi and 83%, respectively. Fig. 4(b) displays xz and yz planes of the single array. Here, the directivity of antenna is more than 9 dBi while the angular width (3 dB) is 40.3 degrees.

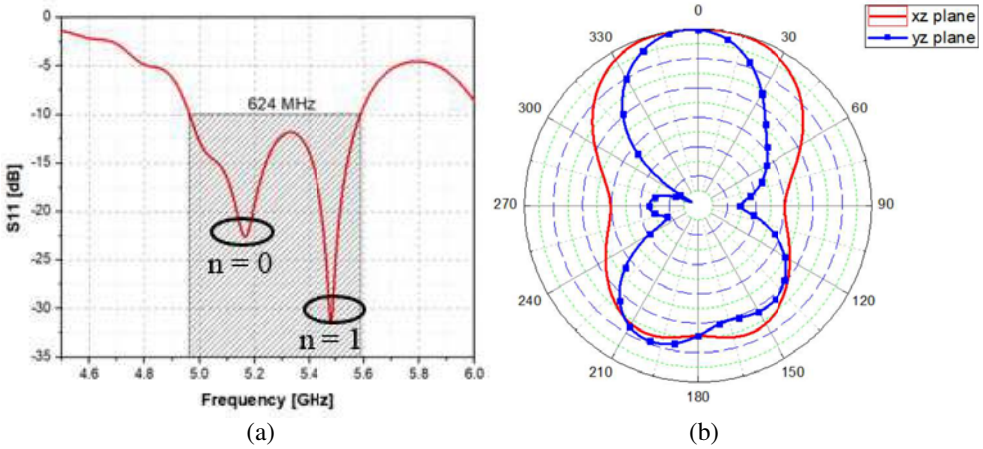

(a) (b)

Figure 4. (a) The reflection coefficient; (b) xz and yz planes of the single antenna.

4.1.2. MIMO Array Antenna

To confirm the influence of the proposed DGS on parameters of the antenna, this paper sets two simulation cases with and without the DGS, and this is illustrated in Fig. 5.

In Fig. 5, we can see that the bandwidth of antenna with the proposed DGS is 300 MHz while this value without DGS is only 130 MHz. In addition, the isolation of antenna is significantly improved when DGS is used. This is shown when the figures with and without DGS are 20 dB and 15 dB, respectively. It is clear that the current redistribution through using DGS allows us to adjust the currents that are concentrated in a specific location while there are limitations at other locations. As a result, the isolation is enhanced. Using DGS not only improves bandwidth and isolation for antenna, but also enhances gain for antenna. This is displayed in Fig. 5(b) when gains of antenna with and without DGS are 9.5 dBi and 8.7 dBi, respectively. Fig. 6 shows the gains of single and MIMO antenna versus the frequency.

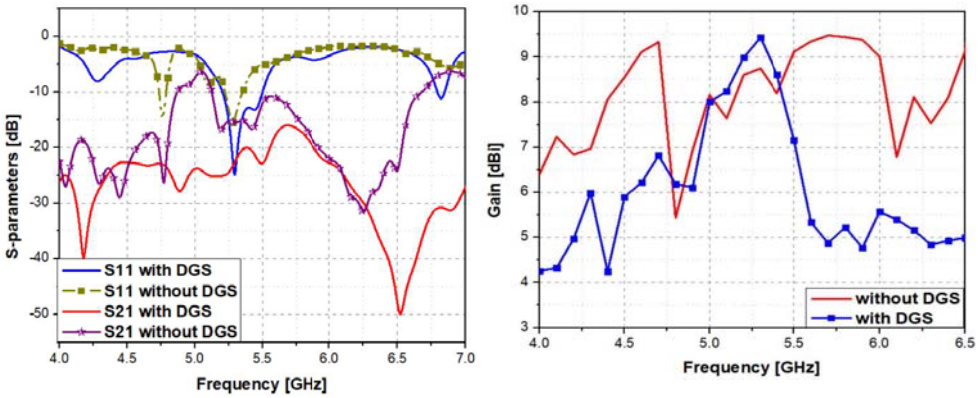

(a) (b)

Figure 5. The parameters of antenna with and without DGS: (a) S-parameters and (b) gain.

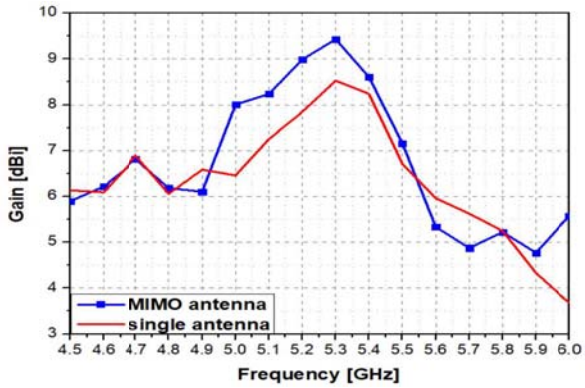

Figure 6. The gains of single and MIMO antenna versus the frequency.

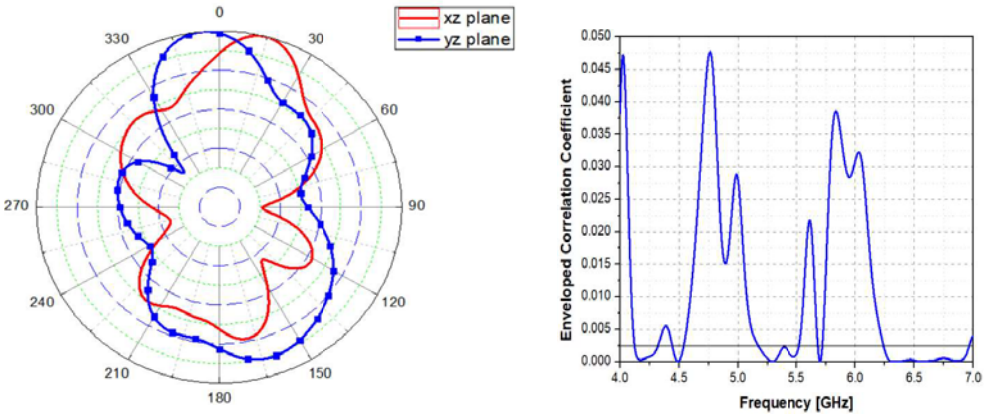

(a) (b)

Figure 7. The planes and ECC of the MIMO antenna.

Moreover, there is an important parameter in MIMO system to determine diversity performance, which is the enveloped correlation coefficient (ECC). Here, ECC is defined as follows [19]:

$$\rho_e = \frac{\left|S_{11}^* S_{12} + S_{21}^* S_{22}\right|^2}{\left(1 - \left|S_{11}\right|^2 - \left|S_{21}\right|^2\right)\left(1 - \left|S_{22}\right|^2 - \left|S_{12}\right|^2\right)} \tag{10}$$

Figure 7 illustrates the planes (including xz and yz) and ECC of the proposed MIMO antenna. The directivity of antenna is 9.7 dBi whereas the angular width (3 dB) is 35 degrees. Besides, while the radiation efficiency of antenna reaches over 93%, the ECC is under 0.0025 (from 5.17 GHz to 5.52 GHz). This shows that there is a high isolation in MIMO antenna.

4.2. Measurement Results

To verify the performance, the prototypes of final MIMO and single antennas with dimensions of 145 $\times$ 88 $\times$ 1.575 mm^3 and 75 $\times$ 82 $\times$ 1.575 mm^3 are fabricated and measured. Fig. 8 illustrates the fabricated samples of the prototypes, which are designed on a Roger RT/DuroidTM 5880 substrate with $h = 1.575$ mm, $\varepsilon_r = 2.2$, and $\tan\delta = 0.0009$. The measured and CST Studio simulated results are shown in Fig. 9 while the results of the pattern measurement are illustrated in Fig. 10. From Fig. 9, we can see that the bandwidths of single array and MIMO array are 570 MHz and 260 MHz, respectively (corresponding to 10.75% and 5%). In addition, the mutual coupling of the MIMO antenna is under -20 dB. There is a large tolerance between measured and simulated results of S_{21}. This difference can be caused from the tolerances in fabrication progress. However, the frequency range for operating of the antenna is still ensured; therefore, this result is acceptable.

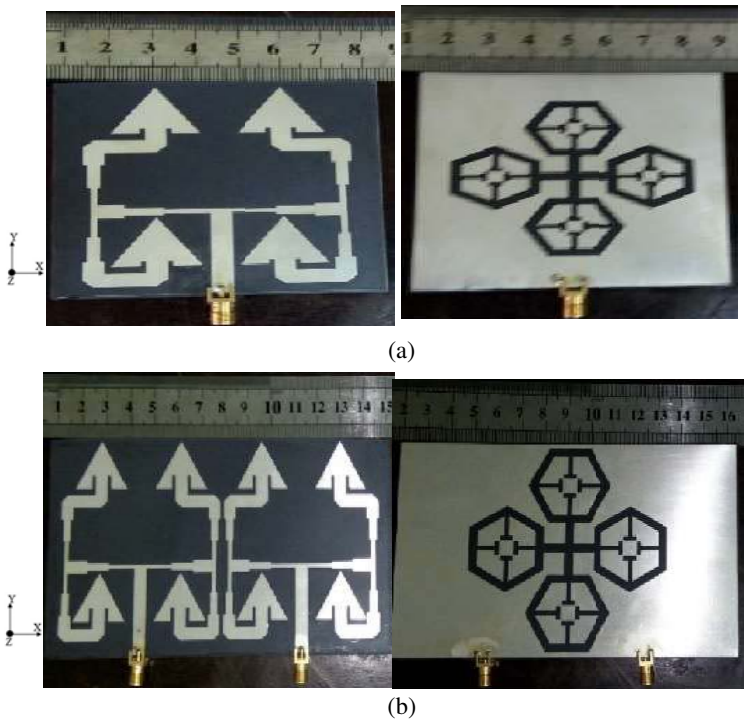

Figure 8. Photograph of fabricated antenna: (a) single array; (b) MIMO array.

The results of the proposed MIMO antenna and the recent MIMO antennas are summarized in Table 3. In [20], although there is a large bandwidth percentage; the isolation of antenna is very high; the gain of antenna is only 6 dBi. Similarly, there is a high isolation in [21], and the gain of antenna is not good (5.3 dBi). In another paper [23], the gain and isolation of antenna are 3.98 dBi and 14 dB, respectively. However, the bandwidth percentage in [23] is quite high with 13%. In contrast, the mutual coupling of antenna in [22] is quite high (13.5 dB), but the gain is better (8 dBi). In another aspect, the size of the proposed antenna is larger than the reference antennas. This is because MIMO antennas of references have only single element while the proposed antenna is an array (including 4 elements). Therefore, the size of the proposed antenna is larger than antennas in references, which is understandable.

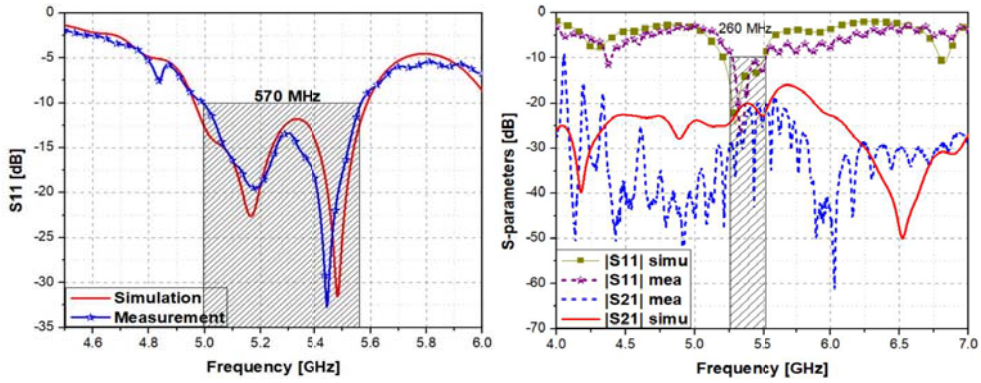

(a) (b)

Figure 9. Measurement results of the S-parameters: (a) single array antenna; (b) MIMO array antenna.

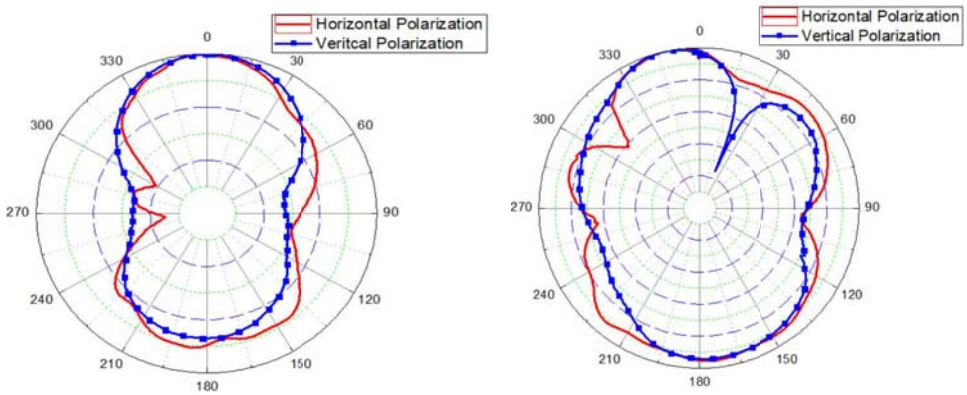

(a) (b)

Figure 10. Measurement results of pattern: (a) single array; (b) MIMO array.

Table 3. Measured result comparison of the proposed MIMO antenna and recent references.

References	[20]	[22]	[21]	[23]	[13]	**My work**
Frequency [GHz]	5.5	2.4	5.8	2.4	2.45	**5.3**
Bandwidth [%]	21.1	9.6	7.8	13	2	**5**
Isolation [dB]	45	13.5	34	17	10	**20**
Radiation efficiency [%]	×	×	×	85	78	**93**
Gain [dBi]	6	8	5.3	3.98	1.26	**9.5**
Size	×	$0.91\lambda \times 0.91\lambda \times 0.17\lambda$	$1.87\lambda \times 0.54\lambda \times 0.029\lambda$	$0.56\lambda \times 0.56\lambda \times 0.0122\lambda$	$0.817\lambda \times 0.41\lambda \times 0.013\lambda$	$\mathbf{2.56\lambda}\times \mathbf{1.55\lambda}\times \mathbf{0.027\lambda}$

5. CONCLUSION

A MIMO antenna using DGS is presented in this paper. The MIMO antenna includes two sets of 2×2 elements, and it is designed at the central frequency of 5.3 GHz. Based on RT5880 with $h = 1.575$ mm, $\varepsilon_r = 2.2$, and $\tan\delta = 0.0009$, and the overall dimension is $145 \times 88 \times 1.575\,\text{mm}^3$. By using the proposed DGS, the gain of antenna achieves the peak gain of 9.5 dBi while the measured bandwidth at -10 dB gets 260 MHz. Moreover, there is a high isolation between elements in array with more 20 dB and a high radiation efficiency of 93%. With the advantages of easy fabrication, low cost, compact size, high gain, and radiation efficiency, the antenna can be widely applied in practice.

REFERENCES

1. Alam, S., M. T. Islam, and H. Arshad, "Gain enhancement of a multiband resonator using defected ground surface on epoxy woven glass material," *The Scientific World Journal*, 2014.
2. Rajawat, A., P. K. Singhal, S. H. Gupta, and C. Jain, "Gain enhancement of microstrip patch antenna using H-shaped defected ground structure," *Progress in Intelligent Computing Techniques: Theory, Practice, and Applications*, 2018.
3. Zheng, Y., et al., "Metamaterial-based patch antenna with wideband RCS reduction and gain enhancement using improved loading method," *IET Microwaves, Antennas & Propagation*, Vol. 11, No. 9, 1183–1189, 2017.
4. Saravanan, M., V. B. Geo, and S. M. Umarani, "Gain enhancement of patch antenna integrated with metamaterial inspired superstrate," *Journal of Electrical Systems and Information Technology*, 2–9, 2018.
5. Kim, J. H., C. H. Ahn, and J. K. Bang, "Antenna gain enhancement using a holey superstrate," *IEEE Transactions on Antennas and Propagation*, Vol. 64, No. 3, 1164–1167, 2016.
6. Cao, W., B. Zhang, A. Liu, T. Yu, D. Guo, and Y. Wei, "Gain enhancement for broadband periodic endfire antenna by using split-ring resonator structures," *IEEE Transactions on Antennas and Propagation*, Vol. 60, No. 7, 3513–3516, 2012.
7. Liu, Z., P. Wang, and Z. Zeng, "Enhancement of the gain for microstrip antennas using negative permeability metamaterial on low temperature co-fired ceramic (LTCC) substrate," *IEEE Antennas and Wireless Propagation Letters*, Vol. 12, 429–432, 2013.
8. Roy, S. and U. Chakraborty, "Gain enhancement of a dual-band WLAN microstrip antenna loaded with diagonal pattern metamaterials," *IET Communications*, Vol. 12, No. 12, 1448–1453, 2018.
9. Khandelwal, M. K., B. K. Kanaujia, and S. Kumar, "Defected ground structure: fundamentals, analysis, and applications in modern wireless trends," *International Journal of Antennas and Propagation*, 1–22, 2017.
10. Dgs, G. S., "Investigation of novel tapered hybrid defected ground structure (DGS)," *International Journal RF and Microwave Computer-Aided Engineering*, 544–550, 2005.
11. Paulraj, A. J., D. A. Gore, R. U. Nabar, and H. Bölcskei, "An overview of MIMO communications — A key to gigabit wireless," *Proceedings of the IEEE*, Vol. 92, No. 2, 198–217, 2004.
12. Pandit, S., A. Mohan, and P. Ray, "A compact four-element MIMO antenna for WLAN applications," *Microwave and Optical Technology Letters*, Vol. 60, No. 2, 289–295, 2018.
13. Sharawi, M. S., et al., "A CSRR loaded MIMO antenna system for ISM band operation," *IEEE Transactions on Antennas and Propagation*, Vol. 61, No. 8, 4265–4274, 2013.
14. Yang, L., S. Yan, and T. Li, "Compact printed four-element MIMO antenna system for LTE/ISM operations," *Progress In Electromagnetics Research Letters*, Vol. 54, 47–53, 2015.
15. Anitha, R., P. V. Vinesh, K. C. Prakash, P. Mohanan, K. Vasudevan, and S. Member, "A compact quad element slotted ground wideband antenna for MIMO applications," *IEEE Transactions on Antennas and Propagation*, Vol. 64, No. 10, 4550–4553, 2016.
16. "Gaussian beam," Online Available: https://en.wikipedia.org/wiki/Gaussian_beam.
17. Bhuiyan, M. D. S. and N. C. Karmakar, "Defected ground structures for microwave applications," *Wiley Encyclopedia of Electrical and Electronics Engineering*, 1–31, 2014.

18. Balanis, C. A., *Antenna theory: Analysis and Design*, 4th Edition, John Wiley & Sons, Inc, Canada, 2016.
19. Blanch, S., J. Romeu, and I. Corbella, "Exact representation of antenna system diversity performance from input parameter description," *Electronics Letters*, Vol. 39, No. 9, 705, 2003.
20. Han, W., X. Zhou, J. Ouyang, Y. Li, R. Long, and F. Yang, "A six-port MIMO antenna system with high isolation for 5 GHz WLAN access points," *IEEE Antennas and Wireless Propagation Letters*, Vol. 13, 880–883, 2014.
21. Malviya, L., R. K. Panigrahi, and M. V. Kartikeyan, "Circularly polarized 2×2 MIMO antenna for WLAN applications," *Progress In Electromagnetics Research C*, Vol. 66, 97–107, 2016.
22. Costa, J. R., E. B. Lima, C. R. Medeiros, and C. A. Fernandes, "Evaluation of a new wideband slot array for MIMO performance enhancement in indoor WLANs," *IEEE Transactions on Antennas and Propagation*, Vol. 59, No. 4, 1200–1206, 2011.
23. Malviya, L. D., R. K. Panigrahi, and M. V. Kartikeyan, "A 2×2 dual-band MIMO antenna with polarization diversity for wireless applications," *Progress In Electromagnetics Research C*, Vol. 61, 91–103, 2016.